

# Diterpene 16-hydroxycleroda-3,13-dien-15,16-olide emerges non-canonical autophagic cell death in doxorubicin-resistant lung cancer

**Wei-Jun Chiu**

National Dong Hwa University

**Shian-Ren Lin**

National Dong Hwa University

**Chia-Jen Wu**

National Dong Hwa University

**Chun-Shu Lin**

National Defense Medical Center

**Prabhakar Busa**

National Dong Hwa University

**Hui Long**

National Dong Hwa University

**Ching-Cheng Chen**

St Mary's Hospital Center

**Feng-Jen Tseng**

Hualien Armed Forces General Hospital

**Ching Feng Weng** (✉ [cwfeng-cwfeng@hotmail.com](mailto:cwfeng-cwfeng@hotmail.com))

Xiamen Medical College

---

## Research article

**Keywords:** 16-hydroxycleroda-3,13-dien-15,16-olide, Non-small cell lung carcinoma, Autophagy, Herbal medicine, Doxorubicin

**Posted Date:** February 25th, 2020

**DOI:** <https://doi.org/10.21203/rs.2.24399/v1>

**License:**  This work is licensed under a Creative Commons Attribution 4.0 International License.

[Read Full License](#)

---

## Abstract

Background: The antitumor activity of HCD has been reported in numerous types of cancers. Moreover, the antitumor of HCD could also be applied in non-small-cell lung cancer (NSCLC) cells and further act on doxorubicin-resistant (Dox-R) of NSCLC cells. The underlying anti-cancer mechanism of HCD on Dox-R versus Dox-sensitive (Dox-S) of A549 cells was under this investigation.

Methods: Cytotoxicity of HCD against two cell lines (Dox-S and Dox-R) were determined via MTT assay, flow cytometry, and Western blot; and further examination of its anti-cancer efficacy in A549-bearing xenograft mice via orthotopic intratrachea (IT) inoculation.

Result: Regardless sensitive and resistant to Dox, HCD could arrest both Dox-S and Dox-R cells at G 2 /M phase without altering the sub-G 1 cycle along with increasing cleaved-PARP. HCD downregulated the mTOR/Akt/PI3K-p85 and PI 3 K-ClassIII/Beclin-1 and upregulated p62/LC3-I/II expressions, further confirmed the cell autophagy after HCD-induced. Morphological observations of the mouse lung sections illustrated that fewer cancer cells accumulated around the trachea while there were less neoplastic activities found in HCD orthotopic treatment mice without liver, kidney and spleen toxicity.

Conclusion: HCD exhibited the chemotherapeutic potential for lung cancer in Dox-resistant cells, suggesting natural autophagic inducer HCD provides a promising clue of new drug discovery and development for lung cancer therapy.

## Background

Lung cancer is the leading cause of cancer death and new diagnosis cases, which the incident and mortality rate in both gender are 218.6 (male incidence), 182.6 (female incidence), 122.7 (male mortality), and 83.1 (female mortality) in 100,000 people, respectively<sup>1</sup>. Lung cancer globally causes 1.8 million cancer death in 2018, which is close to 1 in 5 from all cancer deaths of all cancer sites<sup>1</sup>. In pathological classification, lung cancer could be mainly categorized into 2 groups: small cell lung cancer (SCLC) and non-small-cell lung cancer (NSCLC), which NSCLC includes squamous cell cancer (SCC), adenocarcinoma (AC), large cell cancer, and others<sup>2</sup>. Comparing to SCLC, NSCLC is much higher incidence worldwide, especially SCC and AC, which are gender difference in the highest prevalence of lung cancer type (male, SCC) and (female, AC), respectively<sup>3</sup>. The population of lung cancer patients mainly is distributed between 55 and 74 years old in both gender and the incident rate are cumulative with increasing age<sup>4</sup>. In addition to age, the most-important single risk of lung cancer is cigarette smoking, including tobacco, cannabis, and electronic cigarette delivery system<sup>4</sup>. Moreover, about 10% in males patients in the Western world and unexpectedly up to nearly 40% female patients in Asia reveal no correlation with cigarette smoking<sup>5</sup>. These non-canonical lung cancer cases might be caused by life-styles or environmental toxins such as PM2.5<sup>6</sup>. Accordingly, treating lung cancer, especially NSCLC, is a critical episode for improving human being health and survival.

Clinically, surgery is the first choice for the treating patients before stage III of NSCLC<sup>7</sup>. According to the abovementioned description, elder patients are major population of lung cancer, which post-surgical infection is frequently lower prognosis than younger patients<sup>8</sup>. Therefore, radiotherapy or chemotherapy usually become adjuvant therapy of surgery to improve prognosis<sup>2</sup>. Currently, platinum-based chemotherapeutic drugs (cisplatin, carboplatin), epidermal growth factor receptor inhibitors (EGFRi, e.g., gefitinib), mutated anaplastic lymphoma kinase inhibitors (ALKi, e.g., crizotinib, alectinib), and vascular endothelial growth factor inhibitors (VEGFi, e.g., bevacizumab) are classified as first-line chemotherapy<sup>9</sup>. However, the adverse effects such as hair-loss, nephrotoxicity, and xerosis are often decreased patients' life quality and restricted regimen dose<sup>10,11</sup>.

Remarkably, the nascent structure or origin of some cancer chemotherapeutic drugs in clinical use are naturally derived products, which indicates that natural products could be chemotherapeutic agents without or less adverse effects<sup>12</sup>. Numerous reports have shown that there are many natural compounds that possess lung cancer-treating potential such as berberine from *Coptis chinensis*, which promotes intrinsic apoptosis pathway<sup>13</sup>, matrine from *Sophora flavescens* Ait, gambogic acid from *Garcinia hunburyi*, and prodigiosin from *Serratia marcescens* lead NSCLC cells to the autophagy via generating ROS and consequently result in cell death<sup>14–16</sup>. Hence, new drug discovery and high efficacy with fewer side effects provides an anticipation for curing of lung cancer patients.

*Polyalthia longifolia* belongs to the Annonaceae family and is widely distributed in India, Pakistan, and Sri Lanka which have been used as medications for thousand years<sup>17</sup>. Its traditional-medical indication has assessed in evidence-based approaches for decades and antibacterial, anticancer, and anti-inflammatory activities have been confirmed<sup>18</sup>. 16-hydroxycleroda-3,13-dien-15,16-olide (HCD) is one type diterpene isolated from *P. longifolia* which has reported tumorcidal activity in various cancers such as glioma, oral squamous cell carcinoma (OSCC), and renal cell carcinoma<sup>19,20</sup>. In our previous studies have demonstrated that HCD exerts as an autophagic activator to express antitumor activity in glioma and OSCC cells<sup>21,22</sup>. However, the tumorcidal potential of HCD against NSCLC cells particular in chemo-resistant cancer cells has not been elucidated. Hence, this study aims to evaluate whether HCD implemented any chemotherapeutic potential for lung cancer in doxorubicin-sensitive (Dox-S) and Dox-resistant (Dox-R) of A549 cells, and orthotopic A549-bearing mice model. In addition, the underlying mechanism of HCD-triggered anti-cancer activity would also be investigated.

## Methods

## Materials

The isolation of HCD was previously described<sup>23</sup>. Doxorubicin (Dox) and general-used chemicals were purchased from Sigma-Aldrich (Merck KGaA, Darmstadt, Germany). Reagents and mediums for cell culture were obtained from Thermo-Fisher (Waltham, MA, USA).

## Cell cultures

Human lung cancer cell line A549 (Dox-S, RRID: CVCL\_0023) was obtained from Bioresource Collection and Research Center (BCRC, Hsinchu, Taiwan) and cultured under cultural condition (37 °C, 5% CO<sub>2</sub>, saturated humidity). Culture medium was high-glucose Dulbecco's modified Eagle medium (DMEM-HG) plus 10% FBS and 1% penicillin/streptomycin (PS) which renewed every 2 days. As the cells reached 80% confluence, cells were detached by 0.25% trypsin/EDTA for further experiments. All cell tests were performed within 20 passages to keep uniformity and consistency.

Dox-resistant A549 strain (Dox-R) was derived from parental A549 strain via pulse treatment of Dox. In the beginning, A549 cells were incubated with 2.5 μM of Dox for 24 h. Then culture medium was replaced by new cultural medium and continuously cultured for 1 week. The pulse-treating steps were repeated and Dox concentration was sequentially elevated up to 100 μM. Culture condition of Dox-R was the same as the parental Dox-S.

## Cytotoxicity assay

Cell viability was used for cytotoxicity and determined by an MTT assay<sup>15</sup>. Briefly, 7 × 10<sup>3</sup> cells per well of two cells were inoculated into 96-well plate. Dox or HCD diluted into appropriate concentration were replaced into wells and incubated 24 h under culture condition, respectively. Then, MTT solution was added into well and incubated for additional 4 h. Optical density at 570 nm was measured by Opsys MR™ Microplate Reader (Dynex, Chantilly, VA, USA). Cytotoxicity was denoted by cell viability that calculated from the percentage between the treated and untreated groups. To confirm that HCD-induced the autophagic cell death, 1 and 3 nM of baflomycin A1 (BA1, Santa Cruz Biotechnology, Dallas, TX, USA) was co-treated with 2.5 μM HCD in Dox-S cells and measured changes in cell viability.

## Cell cycle measurements

The process of cell cycle analysis was followed from the literature<sup>15</sup>. Briefly, 7 × 10<sup>4</sup> cells were inoculated into 12-well plate. When cell attached, cells were treated with HCD or Dox for 24 h, respectively. Cells and supernatant were collected by trypsin/EDTA and fixed by ice-cool 70% EtOH/PBS. Before the test, cells were stained with 0.1 mg/mL of propidium iodide for 1 h and detected excitation/emission intensity in each cell at 493/636 nm by Cytomics™ FC500 flow cytometry (Beckman-Coulter, Brea, CA, USA). 1 × 10<sup>4</sup> data points were acquired from each individual sample and plotted the histogram for analyzing cell cycle.

## Western blotting

The protocol of Western blotting was followed the step-in previous study<sup>15</sup>. Briefly, 3.5 × 10<sup>5</sup> cells were seeded into the 6-well and incubated overnight. Using appropriate concentrations of HCD were treated for 24 h, respectively. After treatments, cells were washed with pre-warm PBS and the whole cellular proteins were extracted by RIPA buffer, the debris and supernatant were collected into 1.5 mL eppendorf, and centrifuged at 13000 rpm under 4°C for 30 min. The soluble proteins were separated by sodium dodecyl sulfate (SDS) polyacrylamide gel electrophoresis (PAGE), the gel was transferred to PVDF membrane (GE Healthcare, Chicago, IL, USA), and was blocked by skimmed milk at room temperature (RT) for 1 h. The blocked membranes were cut according to molecular weight, incubated with appropriate 1st antibody at

4°C overnight, and stained with HRP-conjugated 2nd antibody at RT for additional 1 h. The membrane was soaked into enhanced chemiluminescence reagent (EMD Millipore, Burlington, MA, USA) and snapshotted by LAS-3000 image system (Fujifilm, Tokyo, Japan). The stained signals in each membrane were normalized with signal of internal control (GAPDH) and convert to ratio to control.

## In situ xenograft animal model and HCD treatment

Six to eight-week old female C57BL/6 mice, obtained from the National Laboratory Animal Center (Taipei, Taiwan) were used in this test. The feeding regimen of animals was followed by the condition as previously described<sup>15</sup>. The animal experiment protocol was approved by National Dong-Hwa University Animal Ethics and followed the regulation from Guide for the Care and Use of Laboratory Animals”.

C57BL/6 mice were allotted into 8 groups (group 1: untreated; group 2: 10% EtOH; group 3: Dox-S; group 4: Dox-R; group 5: Dox-S plus 0.32 (100 µM) mg/kg B.wt. of HCD; group 6: Dox-R plus 0.32 (400 µM) mg/kg B.wt. of HCD; group 7: Dox-S plus 1.27 mg/kg B.wt. of HCD; and group 8: Dox-R plus 1.27 mg/kg B.wt. of HCD. Each of all treated groups was n = 6). Dox-S and Dox-R cells were collected using trypsin/EDTA followed by centrifuging with 1500 rpm at RT. Before injection, cells were re-suspended in PBS. At day 0, mice in groups 3 to 8 were weighed and anesthetized using 5 mg/mL of pentobarbital and intratrachea (IT) inoculated  $1 \times 10^7$  cells per mouse of two cell lines once per 7 d, respectively. At day 28, 0.32 or 1.27 mg/kg B.wt. of HCD and 10% EtOH were IT injected into the lungs and weighed once per 5 days and ended at day 53. Mice were sacrificed by CO<sub>2</sub> asphyxiation at day 28, 35, and 53, respectively. Liver, kidney, spleen, and human tumors in mice lungs were collected for slicing. Cytotoxicity of HCD and the migrations of tumor were observed by H&E staining.

## Statistical analysis

The quantified results were presented as mean ± SD for the three independent experiments and analyzed by a one-way ANOVA with Tukey's test for post-Hoc test. All statistical procedures were performed with GraphPad Prism Ver 7.04 (GraphPad Software Inc., La Jolla, CA, USA). Significant differences (p < 0.05) between the control and treated group were marked in “\*”.

## Result

### Cytotoxicity of HCD in Dox-S and Dox-R cells

To determine the cytotoxicity of HCD, Dox-S and Dox-R cells were treated with various concentrations of HCD (1.0–20 µM) to measure the cell viability in two cells. Cell viability in both cells were dose-dependently decreased with increased concentrations of HCD, which IC<sub>50</sub> was 20 µM in both Dox-S and Dox-R, respectively (Fig. 1A). The IC<sub>50</sub> of Dox against two cell lines was 10 µM, which indicated that the cytotoxicity of HCD was less than that of Dox (Fig. 1B). The subsequent experiments were performed to study the primary causes of HCD-induced cell death.

# Analyzing apoptosis and autophagy markers after HCD treatments

Next, apoptotic and autophagic markers were applied in two cells to determine the type of cell death. In cell cycle analysis, sub-G<sub>1</sub> phase was not significantly increased in both cell lines under HCD treatment (Fig. 2). When the determination of cell cycle distribution in Dox-R to Dox-S cells under Dox-treatment, Sub-G<sub>1</sub> was significantly increased from 1.3 ± 0.3% (Dox-R) and 1.6 ± 0.2% (Dox-S) at untreated control to 6.5 ± 0.6% (Dox-R) and 9.9 ± 0.8% (Dox-S) at 20 µM of Dox ( $P < 0.05$ ). This result revealed that cell death characteristics between HCD and Dox were speculated with the different fashion and it seems that Dox was associated with apoptosis whereas HCD was not. Interestingly, the apoptotic cell marker, cleaved-PARP (C-PARP) level in Dox-R cells were significantly increased after 2.5 and 25 µM of HCD treatment (Fig. 3A). In Dox-S cells, similar pattern of C-PARP levels could be observed, whereas C-PARP level at 25 µM of HCD treatment was not significantly higher than that of the control (Fig. 3B). On the other hand, the protein levels of autophagic markers LC3-II and p62 were significantly increased, which expression pattern of LC3-II was opposite with C-PARP (Figs. 3A&B). Combining the protein levels of apoptotic and autophagic markers, both apoptosis and autophagy were involved in HCD-induced cell death, and autophagic cell death might be more dominant than apoptosis. To further confirm that HCD could cause autophagic cell death, 1 & 3 nM of baflomycin A1 (BA1) was co-treated with 2.5 µM HCD and then measured the change of cell viability. HCD-induced cell death could be reversed by BA1 (Fig. 3C). These results directly indicated that autophagy was the main character of HCD-induced cell death. Next, the underlying mechanism of HCD-induced autophagic cell death was evaluated.

## Underlying mechanism of HCD-induced cell death in two cell lines

To investigate in more detail HCD-induced autophagic cell death, the upstream and downstream proteins in autophagic regulation pathways were evaluated. In autophagic activator Beclin-1 and PI3K-ClassIII, the change patterns of the two cell lines were different. In Dox-R, PI3K-ClassIII was down-regulated at 2.5 µM HCD and decreased with the increased HCD concentrations, while Beclin-1 expression was inversely correlated with HCD concentrations (Fig. 4A). In contrast to Dox-S cells, expression pattern of PI3K-ClassIII in Dox-R was up-regulated at 2.5 µM HCD and down-regulated at 25 µM of HCD. The expression patterns of Beclin-1 were down-regulated with the elevation of HCD concentrations (Fig. 4B). The reduce of Beclin-1 expression was only observed at 25 µM of HCD treatment in Dox-S cells (Fig. 4B). Different autophagic activator pattern with similar consequence indicated that autophagic cell death in both cells might be through Beclin-1/PI3K-ClassIII-independent pathway.

To unveil the change of upstream regulators, the expression levels of mTOR, Akt, and p38 were next determined. In Dox-R cells, mTOR expression was up-regulated at 2.5 µM HCD and decreased in increase of HCD concentrations, especially at 25 µM HCD treatment, the expression level of mTOR was almost abolished (Fig. 4C). Similar pattern could be found in Dox-S cells, which all three proteins were down-

regulated after HCD treatment (Fig. 4D). Taken above results into considerations, HCD might induce the autophagy through down-regulation of Akt/PI3K-p38/mTOR signaling pathway and subsequently resulting in stimulation of Beclin-1/PI3K-ClassIII-independent autophagy pathway. Finally, orthotopic A549-bearing mice model was employed to measure antitumor activity of HCD *in vivo*.

## Effect of HCD on cancer-inoculating animal model

To further determine the anticancer activity of lung cancer *in vivo*, two cancer cells were firstly intratracheal (IT) inoculated into mice lungs. When compared to normal mice lungs and 10% EtOH injection (solvent control), cancer cell-bearing mice lungs showed more cell accumulation around the trachea, which indicated that cancer cells were successfully inoculated (Figs. 6A-D). After IT injection with 0.32 & 1.27 mg/kg B. wt of HCD, cell invasion around the blood vessels and accumulated around the trachea was prominent abrogation, which revealed that HCD could inhibit lung cancer progression *in vivo* (Figs. 6E-H). Also, the body weights of IT-HCD mice were not significantly different during treatments, which revealed that IT injection of HCD would not cause significant acute toxicity during regimen (Fig. 5). No significant difference was observed in the histo-section of liver, kidney, and spleen among treatments when compared to the untreated control (data not shown). *In vivo* results clearly exhibited treating potential of HCD in applying to NSCLC cancer treatment.

## Discussion

In this study, HCD-treating potential of NSCLC was assessed from *in vitro* assay to *in vivo* test. The results clearly indicated that HCD could simultaneously induce apoptosis and autophagy in both Dox-S and Dox-R cells via down-regulating PI<sub>3</sub>K/Akt/mTOR signaling pathway and led to non-canonical autophagic activation. Interestingly, both apoptosis and autophagy were activated in single NSCLC population, whereas the autophagy was predominant. Finally, HCD could reduce orthotopic xenograft NSCLC cells growth and without visible acute toxicity during regimen.

During exploring anticancer mechanism of HCD, duality of apoptosis/autophagy could be observed in single NSCLC population at one treatment. This interesting phenomenon hinders physiological polymorphism of commercial cell lines in cellular levels. Previously, similar phenomenon could be found in prodigiosin (PG)/Dox synergistic study in OSCC cells, and PG against NSCLC cells<sup>15,24</sup>. However, the discussion of this phenomenon was rare. The detail mechanism and its effect on oncology or translational medicine research needs to be extensive reports for making conclusion.

Earlier heterotopic xenograft reports have demonstrated that BALB/c-nude mice are broadly used to build lung cancer model via back or trunk subcutaneous injection with lung cancer cells<sup>25</sup>; or are implanted into the footpad of C57/BL6 via imitation of patients with lung cancer<sup>26</sup> for evaluating the efficacy of treatments. Nevertheless, heterotopic xenograft is easily monitoring tumor growth, the microenvironment of tumor growth has still far distance than orthotopic xenograft, especially in preclinical drug test<sup>27</sup>. Nowadays, orthotopic xenograft model for various cancer types including osteosarcoma, prostate cancer,

retinoblastoma, lung cancer, and melanoma have been constructed, and the results from orthotopic xenograft gain an insight into importance of tumorigenesis or anti-tumor<sup>28–30</sup>. However, most orthotopic xenograft model is not easy to monitor the pathological progress than heterotopic xenograft because of hard to monitor interior or deep body site. One reliable approach to overcome this disadvantage is fluorescent labeling on tumor cells and monitoring fluorescent distribution by in vivo imaging system (IVIS) or confocal microscope<sup>31</sup>. In the future, orthotopic xenograft with fashionable monitor system including nano-particle would take into more importance in cancer biology study than heterotopic xenograft.

HCD is firstly identified at 2000 by Chen et al.<sup>23</sup>. After almost two decades' study, antitumor activity of HCD has only partially investigated. In chronic myeloid leukemia cells, HCD causes the apoptosis by two phases: reducing growth-factor-related signaling such as PI3K and aurora B, and reactivating polycomb-repressive protein 2 (PRC2) which modulates histone methylation level and silent/activates pro/anti/apoptotic proteins<sup>32,33</sup>. In renal carcinoma cells, HCD could not only down-regulate the growth-factor-mediated signaling, which leads to intrinsic apoptosis, but also inactivate focal adhesion assembly related signaling and induces anoikis<sup>19</sup>. Using molecular docking, Thiagarajan et al.<sup>34</sup> have found that HCD could affect focal adhesion kinase (FAK) activity via block the autophosphorylation site of FAK. In OSCC and glioma cells studies, HCD triggers autophagic cell death via non-canonical autophagy pathway, which is associated with this study. In exploring detail mechanism, HCD-induced autophagy is triggered by up-regulation of AMPK and down-regulation of Akt-associated signaling in OSCC<sup>22</sup>. In glioma cells, HCD promotes ROS generation which leads to ER stress and results in activation of autophagy<sup>21</sup>. For breast cancer, HCD potentiates tamoxifen-induced cell death in both ER-positive and -negative breast cells via enhancing extracellular apoptotic signaling<sup>35</sup>. In the present study is the first report about treating efficacy of HCD in Dox-S and Dox-R of NSCLC cells. It could explore new trend study for discovering new antitumor function of HCD to curing other types of cancer.

Interestingly, Western blotting results showed that PI3K-ClassIII and Beclin-1 were down-regulated after HCD treatment. Of note, Beclin-1 and PI3K-ClassIII are essential for autophagosome formation. Beclin-1 is the member of autophagosome membrane protein, and PI3K-ClassIII can produce phosphatidylinositol-3-phosphate (PI3P) that forms autophagosome membrane<sup>36</sup>. However, cumulative studies might also demonstrate the existence of alternative autophagy pathways in natural compound treatment for various cancer cells i.e. carnosol in triple-negative breast cancer cells, resveratrol in breast cancer cells, and obatoclax in colorectal cancer cells<sup>37–40</sup>. These natural compounds have activated autophagy and induced apoptosis because Beclin-1 plays a critical role in autophagy/apoptosis crosstalk<sup>41</sup>. Although DNA fragmentation failed to be observed in HCD-treated lung cancer cells, cleaved-PARP was significantly increased in HCD-treated cells and hints at minor apoptosis in lung cancer cells (Fig. 3). Unexpectedly, the up-regulation of cleaved-PARP and LC3-II could be simultaneously observed. It indicated the presence of dual autophagic/apoptotic activation and polymorphism in cell population.

## Conclusion

According all the results, HCD could induce autophagy of both Dox-S and Dox-R cells; and autophagic cell death of HCD-triggered might be through PI3K-ClassIII/Beclin-1-independent signaling pathway. Hence, HCD compound provides a novel approach for the treatment of human tumors. After HCD treatment, there are less neoplastic activities in mice with lung cancer inoculation. Overall, our findings shed light on the autophagic effect of HCD on Dox-S and Dox-R of lung cancer cells through in vitro and in vivo experiments. These results demonstrated that HCD has a favorable medicine value as a potential candidate against cancer disease particular in lung cancer.

## Abbreviations

Adenocarcinoma (AC); Baflomycin A1 (BA1); Doxorubicin (Dox); Dox-resistant (Dox-R); Dox-sensitive (Dox-S); epidermal growth factor receptor inhibitors (EGFRi); focal adhesion kinase (FAK); 16-hydroxycycloda-3,13-dien-15,16-olide (HCD); intratrachea (IT); in vivo imaging system (IVIS); mutated anaplastic lymphoma kinase inhibitors (ALKi); non-small-cell lung cancer (NSCLC); oral squamous cell carcinoma (OSCC); phosphatidylinositol-3-phosphate (PI3P); polycomb-repressive protein 2 (PRC2); prodigiosin (PG); small cell lung cancer (SCLC); squamous cell cancer (SCC); vascular endothelial growth factor inhibitors (VEGFi).

## Declarations

Ethics approval is found in Methods. No applicable in consent to subject participant, consent for publication, and funding. The authors declare no any financial and non-financial competing interests.

### Competing interests

The authors declare no any competing interests.

### Availability of data and material

All data and materials are available once request.

### Author Contributions

Conceptualization, C.F. and M.D.; methodology, C.J. and H.; software, Busa and F.J.; validation, Busa, C.S., and C.C.; formal analysis, S.R. and H.; investigation, W.J.; resources, C.F. and F.J.; writing—original draft preparation, W.J., S.R., and C.C.; writing—review and editing, C.J. and C.S.; funding acquisition, C.F. All authors have read and approved the manuscript.

### Acknowledgments

We sincerely thank Prof. Yaw-Syan Fu and Mr. Sheng-I Lue from Kaohsiung Medical University who gave valuable help in preparations and observations of the staining section.

## References

1. Bray F, Ferlay J, Soerjomataram I, Siegel RL, Torre LA, Jemal A. Global cancer statistics 2018: GLOBOCAN estimates of incidence and mortality worldwide for 36 cancers in 185 countries. *CA Cancer J Clin.* 2018;68(6):394-424.
2. National Cancer Institute. Non-Small Cell Lung Cancer Treatment (PDQ(R)): Health Professional Version. In: *PDQ Cancer Information Summaries*. Bethesda (MD)2002.
3. Cheng TY, Cramb SM, Baade PD, Youlden DR, Nwogu C, Reid ME. The International Epidemiology of Lung Cancer: Latest Trends, Disparities, and Tumor Characteristics. *J Thorac Oncol.* 2016;11(10):1653-1671.
4. de Groot PM, Wu CC, Carter BW, Munden RF. The epidemiology of lung cancer. *Transl Lung Cancer Res.* 2018;7(3):220-233.
5. Gazdar AF, Zhou C. 4 - Lung Cancer in Never-Smokers: A Different Disease. In: Pass HI, Ball D, Scagliotti GV, eds. *IASLC Thoracic Oncology (Second Edition)*. Philadelphia: Content Repository Only!; 2018:23-29.e23.
6. Huang F, Pan B, Wu J, Chen E, Chen L. Relationship between exposure to PM2.5 and lung cancer incidence and mortality: A meta-analysis. *Oncotarget.* 2017;8(26):43322-43331.
7. Brunelli A, Postmus PE. 26 - Preoperative Functional Evaluation of the Surgical Candidate. In: Pass HI, Ball D, Scagliotti GV, eds. *IASLC Thoracic Oncology (Second Edition)*. Philadelphia: Content Repository Only!; 2018:265-273.e263.
8. Venuta F, Diso D, Onorati I, Anile M, Mantovani S, Rendina EA. Lung cancer in elderly patients. *J Thorac Dis.* 2016;8(Suppl 11):S908-S914.
9. Ramalingam SS, Pillai RN, Reinmuth N, Reck M. 44 - Frontline Systemic Therapy Options in Nonsmall Cell Lung Cancer. In: Pass HI, Ball D, Scagliotti GV, eds. *IASLC Thoracic Oncology (Second Edition)*. Philadelphia: Content Repository Only!; 2018:418-433.e416.
10. Manohar S, Leung N. Cisplatin nephrotoxicity: a review of the literature. *J Nephrol.* 2018;31(1):15-25.
11. Izzedine H, Perazella MA. Adverse kidney effects of epidermal growth factor receptor inhibitors. *Nephrol Dial Transplant.* 2017;32(7):1089-1097.
12. Lin SR, Fu YS, Tsai MJ, Cheng H, Weng CF. Natural Compounds from Herbs that can Potentially Execute as Autophagy Inducers for Cancer Therapy. *Int J Mol Sci.* 2017;18(7):e1412.
13. Li J, Liu F, Jiang S, et al. Berberine hydrochloride inhibits cell proliferation and promotes apoptosis of non-small cell lung cancer via the suppression of the MMP2 and Bcl-2/Bax signaling pathways. *Oncol Lett.* 2018;15(5):7409-7414.
14. Zou Y, Sarem M, Xiang S, Hu H, Xu W, Shastri VP. Autophagy inhibition enhances Matrine derivative MASMA induced apoptosis in cancer cells via a mechanism involving reactive oxygen species-mediated PI3K/Akt/mTOR and Erk/p38 signaling. *BMC Cancer.* 2019;19(1):949.
15. Chiu WJ, Lin SR, Chen YH, Tsai MJ, Leong MK, Weng CF. Prodigiosin-Emerged PI3K/Beclin-1-Independent Pathway Elicits Autophagic Cell Death in Doxorubicin-Sensitive and -Resistant Lung

Cancer. *J Clin Med.* 2018;7(10):pii: E321.

16. Ye L, Zhou J, Zhao W, Jiao P, Ren G, Wang S. Gambogic acid-induced autophagy in nonsmall cell lung cancer NCI-H441 cells through a reactive oxygen species pathway. *J Cancer Res Ther.* 2018;14(Supplement):S942-S947.
17. Vijayarathna S, Oon CE, Chen Y, Kanwar JR, Sasidharan S. Polyalthia longifolia Methanolic Leaf Extracts (PLME) induce apoptosis, cell cycle arrest and mitochondrial potential depolarization by possibly modulating the redox status in hela cells. *Biomed Pharmacother.* 2017;89:499-514.
18. Yao LJ, Jalil J, Attiq A, Hui CC, Zakaria NA. The medicinal uses, toxicities and anti-inflammatory activity of Polyalthia species (Annonaceae). *J Ethnopharmacol.* 2019;229:303-325.
19. Chen YC, Huang BM, Lee WC, Chen YC. 16-Hydroxycleroda-3,13-dien-15,16-oxide induces anoikis in human renal cell carcinoma cells: involvement of focal adhesion disassembly and signaling. *Oncotargets Ther.* 2018;11:7679-7690.
20. Liu C, Lee WC, Huang BM, Chia YC, Chen YC, Chen YC. 16-Hydroxycleroda-3, 13-dien-15, 16-oxide inhibits the proliferation and induces mitochondrial-dependent apoptosis through Akt, mTOR, and MEK-ERK pathways in human renal carcinoma cells. *Phytomedicine.* 2017;36:95-107.
21. Thiagarajan V, Sivalingam KS, Viswanadha VP, Weng CF. 16-hydroxy-cleroda-3,13-dien-16,15-oxide induced glioma cell autophagy via ROS generation and activation of p38 MAPK and ERK-1/2. *Environ Toxicol Pharmacol.* 2016;45:202-211.
22. Cheng MF, Lin SR, Tseng FJ, et al. The autophagic inhibition oral squamous cell carcinoma cancer growth of 16-hydroxy-cleroda-3,14-dine-15,16-oxide. *Oncotarget.* 2017;8(45):78379-78396.
23. Chen CY, Chang FR, Shih YC, et al. Cytotoxic constituents of *Polyalthia longifolia* var. pendula. *J Nat Prod.* 2000;63(11):1475-1478.
24. Lin SR, Weng CF. PG-Priming Enhances Doxorubicin Influx to Trigger Necrotic and Autophagic Cell Death in Oral Squamous Cell Carcinoma. *J Clin Med.* 2018;7(10):pii: E375.
25. Zheng MF, Shen SY, Huang WD. DCA increases the antitumor effects of capecitabine in a mouse B16 melanoma allograft and a human non-small cell lung cancer A549 xenograft. *Cancer Chemother Pharmacol.* 2013;72(5):1031-1041.
26. Thotala D, Craft JM, Ferraro DJ, et al. Cytosolic phospholipaseA2 inhibition with PLA-695 radiosensitizes tumors in lung cancer animal models. *PLoS One.* 2013;8(7):e69688.
27. Hoffman RM, Murakami T, Kawaguchi K, et al. High Efficacy of Recombinant Methioninase on Patient-Derived Orthotopic Xenograft (PDOX) Mouse Models of Cancer. In: *Methionine Dependence of Cancer and Aging.* 2019:149-161.
28. Hoffman R. Patient-Derived Orthotopic Xenograft (PDOX) Models of Melanoma. *Int J Mol Sci.* 2017;18(9):pii: E1875.
29. Higuchi T, Miyake K, Oshiro H, et al. Trabectedin and irinotecan combination regresses a cisplatin-resistant osteosarcoma in a patient-derived orthotopic xenograft nude-mouse model. *Biochem Biophys Res Commun.* 2019:pii: S0006-0291X(0019)30598-30594.

30. Civit L, Theodorou I, Frey F, et al. Targeting hormone refractory prostate cancer by in vivo selected DNA libraries in an orthotopic xenograft mouse model. *Sci Rep.* 2019;9(1):4976.
31. Suetsugu A, Shimizu M, Saji S, Moriwaki H, Hoffman RM. Visualizing the Tumor Microenvironment by Color-coded Imaging in Orthotopic Mouse Models of Cancer. *Anticancer Res.* 2018;38(4):1847-1857.
32. Lin YH, Lee CC, Chang FR, Chang WH, Wu YC, Chang JG. 16-hydroxycleroda-3,13-dien-15,16-oxide regulates the expression of histone-modifying enzymes PRC2 complex and induces apoptosis in CML K562 cells. *Life Sci.* 2011;89(23-24):886-895.
33. Lin YH, Lee CC, Chan WL, Chang WH, Wu YC, Chang JG. 16-Hydroxycleroda-3,13-dien-15,16-oxide deregulates PI3K and Aurora B activities that involve in cancer cell apoptosis. *Toxicology.* 2011;285(1-2):72-80.
34. Thiagarajan V, Lin SH, Chia YC, Weng CF. A novel inhibitor, 16-hydroxy-cleroda-3,13-dien-16,15-oxide, blocks the autophosphorylation site of focal adhesion kinase (Y397) by molecular docking. *Biochim Biophys Acta.* 2013;1830(8):4091-4101.
35. Velmurugan BK, Wang PC, Weng CF. 16-Hydroxycleroda-3,13-dien-15,16-oxide and N-Methyl-Actinodaphine Potentiate Tamoxifen-Induced Cell Death in Breast Cancer. *Molecules.* 2018;23(8):E1966.
36. Menon MB, Dhamija S. Beclin 1 Phosphorylation - at the Center of Autophagy Regulation. *Front Cell Dev Biol.* 2018;6:137.
37. Al Dhaheri Y, Attoub S, Ramadan G, et al. Carnosol induces ROS-mediated beclin1-independent autophagy and apoptosis in triple negative breast cancer. *PLoS One.* 2014;9(10):e109630.
38. Scarlatti F, Maffei R, Beau I, Codogno P, Ghidoni R. Role of non-canonical Beclin 1-independent autophagy in cell death induced by resveratrol in human breast cancer cells. *Cell Death Differ.* 2008;15(8):1318-1329.
39. Koehler BC, Jassowicz A, Scherr AL, et al. Pan-Bcl-2 inhibitor Obatoclax is a potent late stage autophagy inhibitor in colorectal cancer cells independent of canonical autophagy signaling. *BMC Cancer.* 2015;15(1):919.
40. Diederich M, Cerella C. Non-canonical programmed cell death mechanisms triggered by natural compounds. *Semin Cancer Biol.* 2016;40-41:4-34.
41. Li M, Gao P, Zhang J. Crosstalk between Autophagy and Apoptosis: Potential and Emerging Therapeutic Targets for Cardiac Diseases. *Int J Mol Sci.* 2016;17(3):332.

## Figures

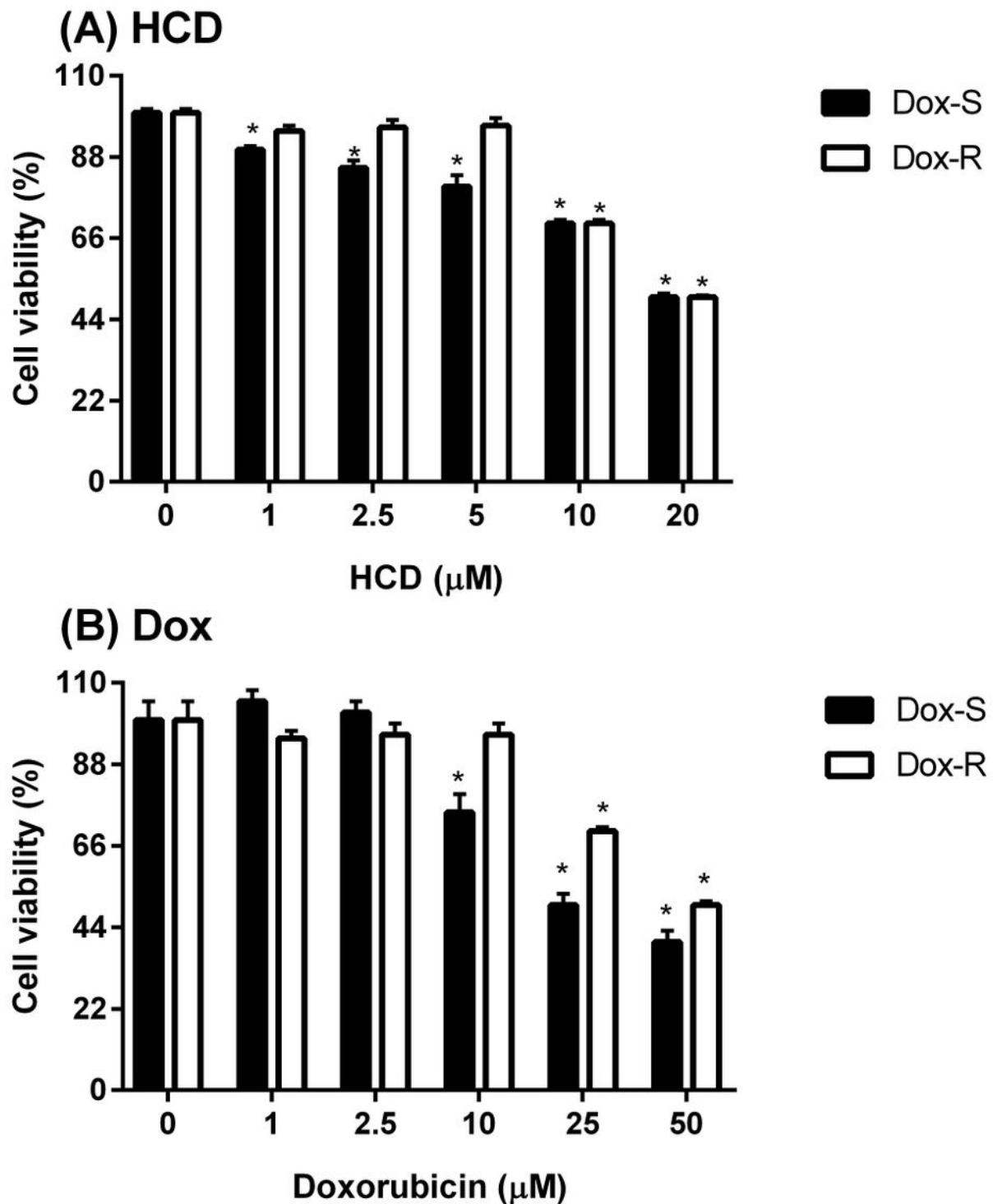


**Figure 1**

The cell viability of Dox-R and Dox-S of A549 cells after HCD and doxorubicin (Dox) treatments. Dox-R and Dox-S cells were treated with various concentrations ( $\mu\text{M}$ ) of (A) HCD and (B) Dox for 24 h, respectively. All the data present as the mean  $\pm$  SD with triplicate determinations in three independent experiments. \*  $P < 0.05$  as compared with the untreated control (0  $\mu\text{M}$ ).

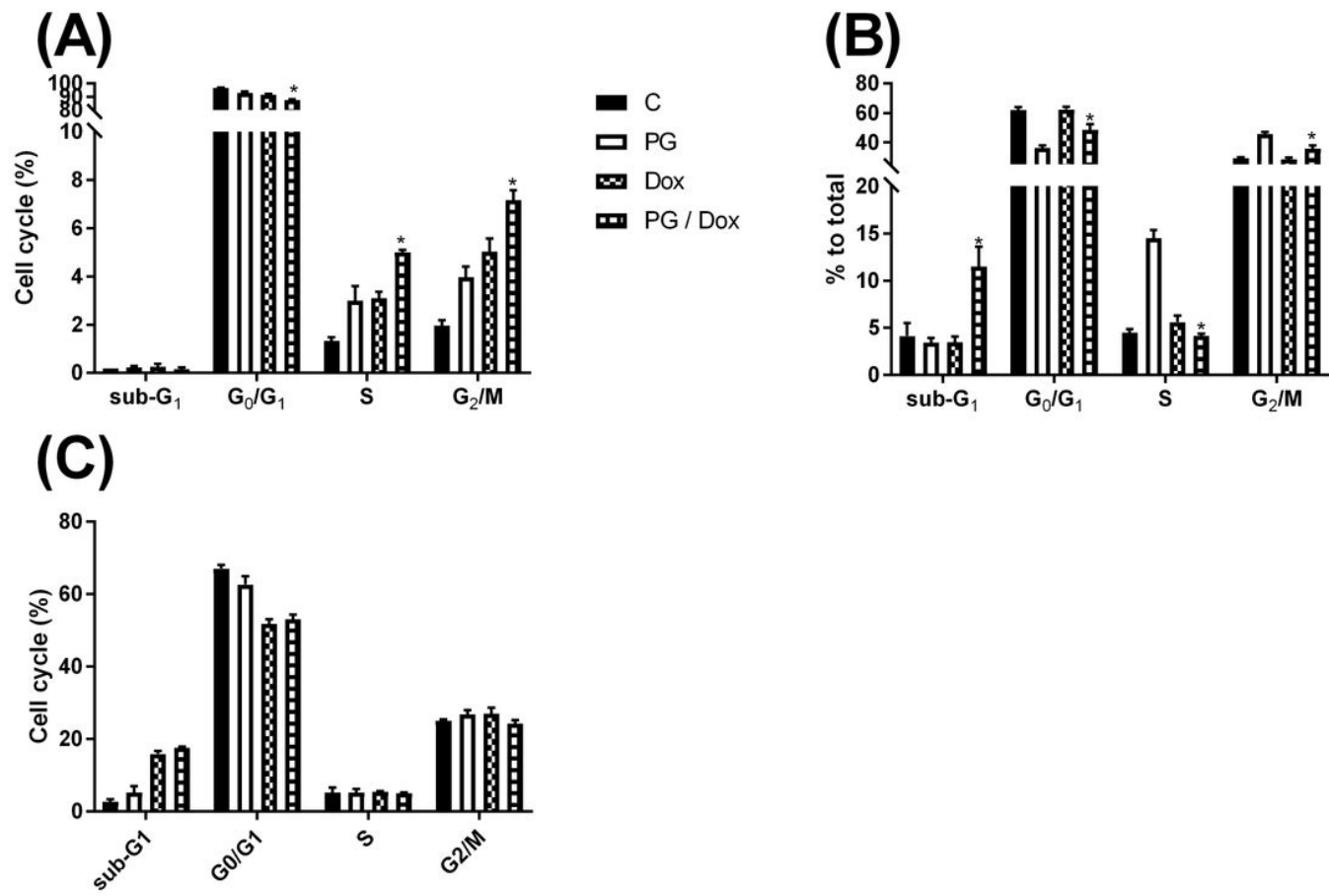


**Figure 2**

Change of cell cycle in Dox-R and Dox-S of A549 cells after HCD treatments. (A) Dox-R and (B) Dox-S cells were treated with HCD for 24 h and detected DNA content within cells. \* P < 0.05, NS not significant compared with the untreated control (0 µM).

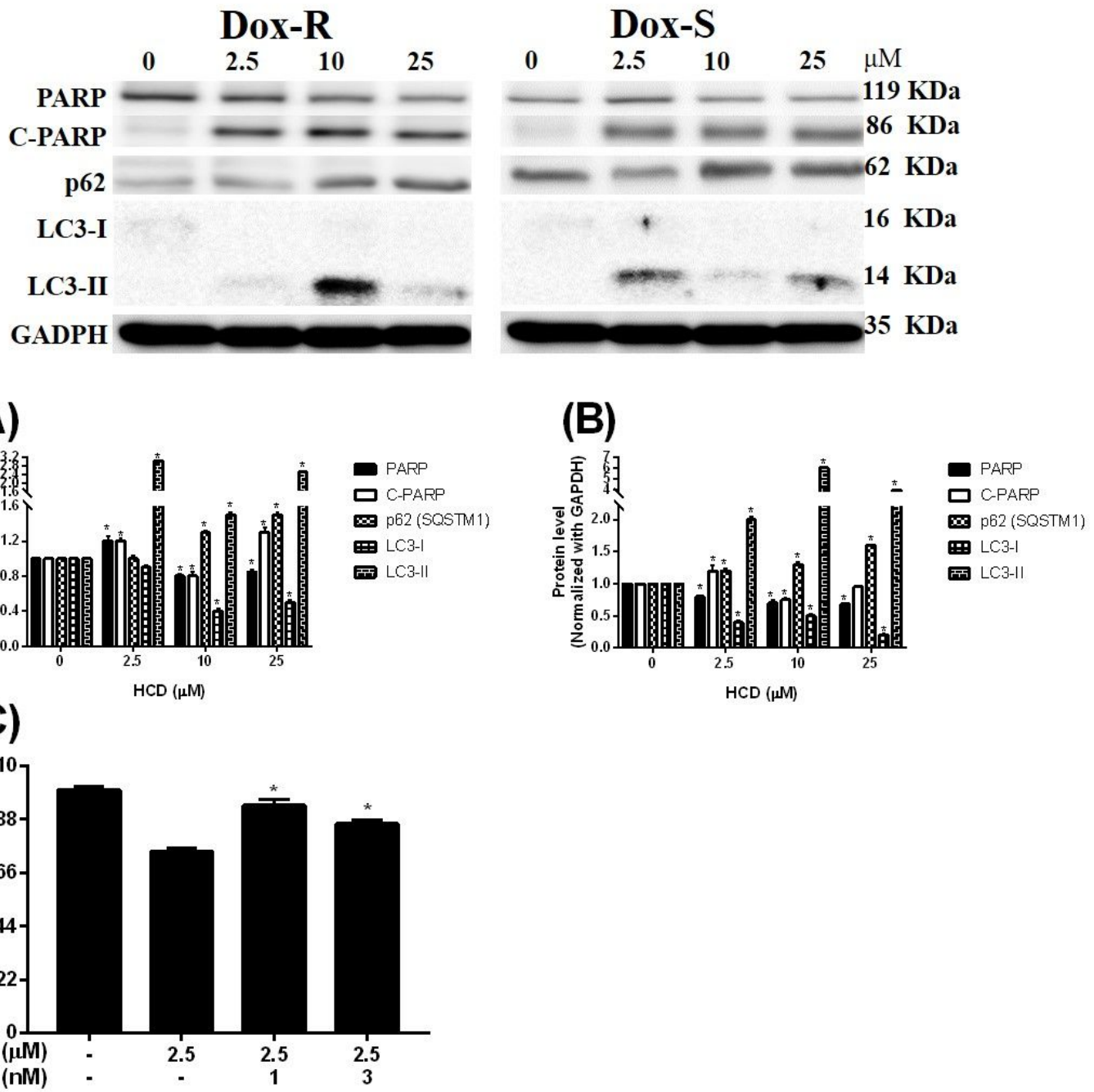


**Figure 3**

Protein level change of autophagic and apoptotic markers in Dox-S and Dox-R of A549 cells. (A) Dox-R and (B) Dox-S cells were treated with HCD and the protein levels were measured by Western blotting. \*  $P < 0.05$  as compared with untreated control. (C) Alteration of cell viability in HCD combined baflomycin A1. HCD was mixed with 1 or 3 nM of baflomycin A1 (BA1) to treat Dox-S cells for 24 h. \*  $P < 0.05$  as compared with HCD alone.

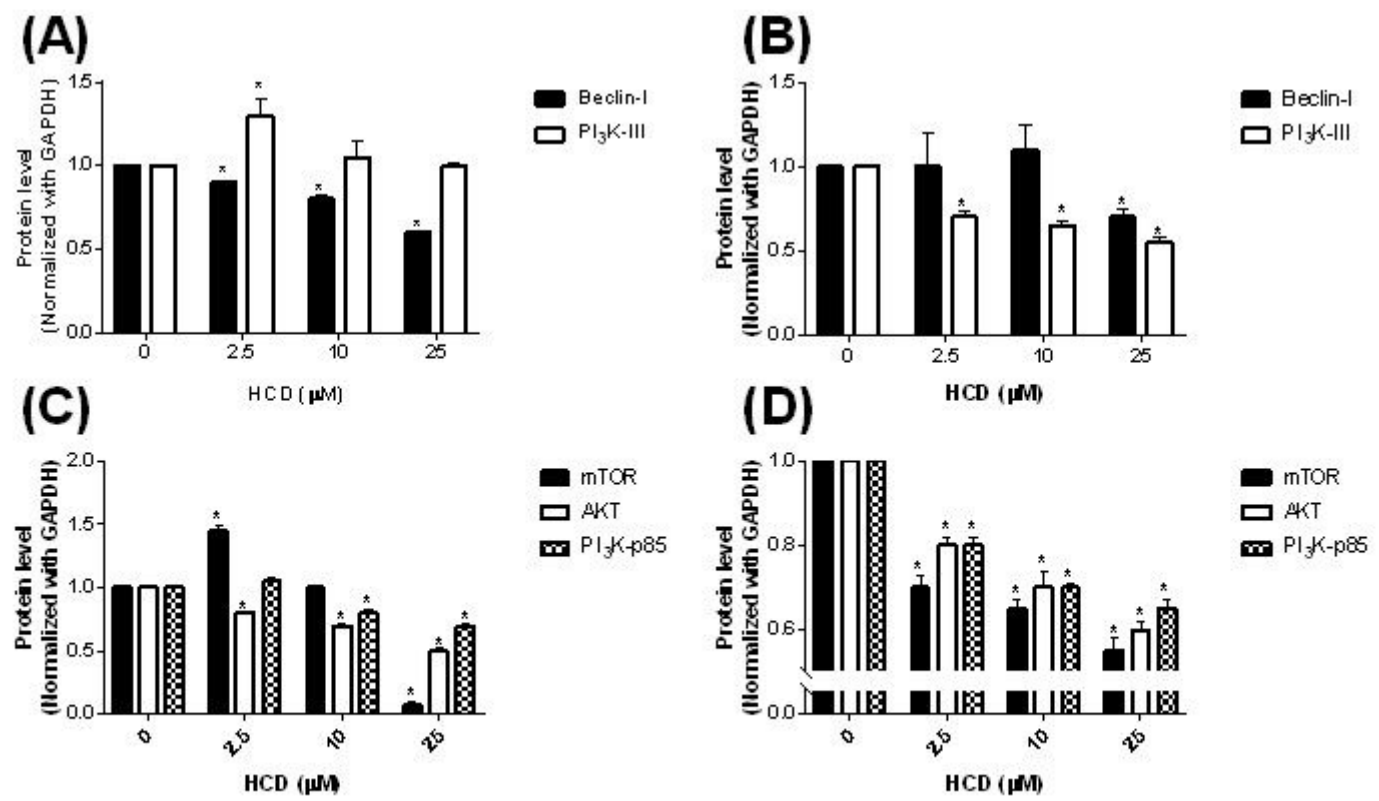
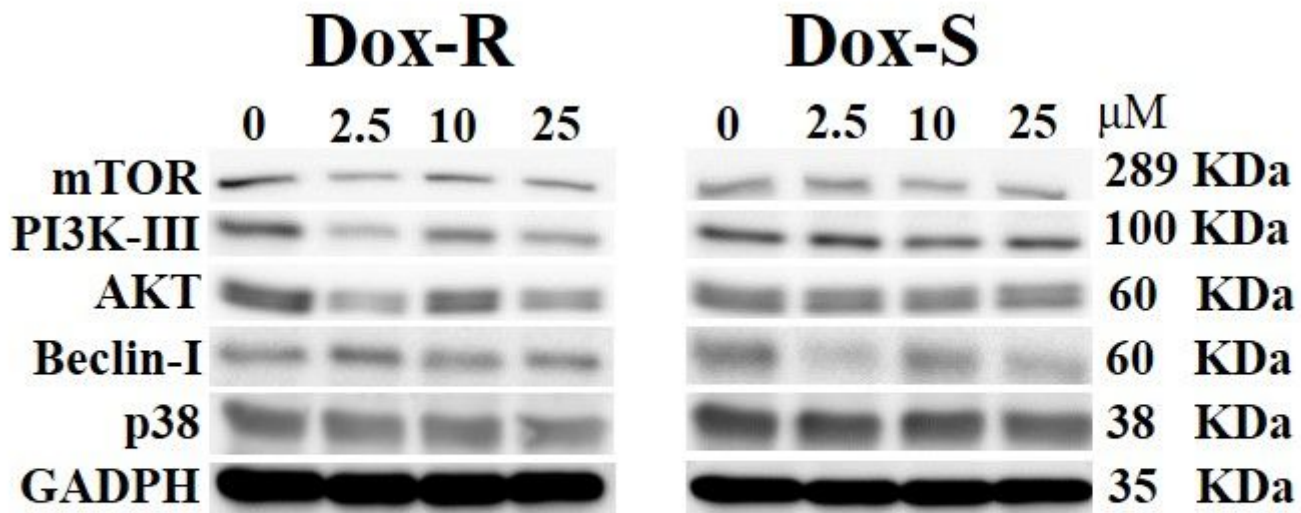


**Figure 4**

Protein level of autophagic regulators in Dox-S and Dox-R of A549 cells. Beclin-1/PI3K-III levels in (A) Dox-R and (B) Dox-S, and mTOR/Akt/p38 levels in (C) Dox-R and (D) Dox-S were measured through Western blotting and quantified. \* P< 0.05 as compared with untreated control.

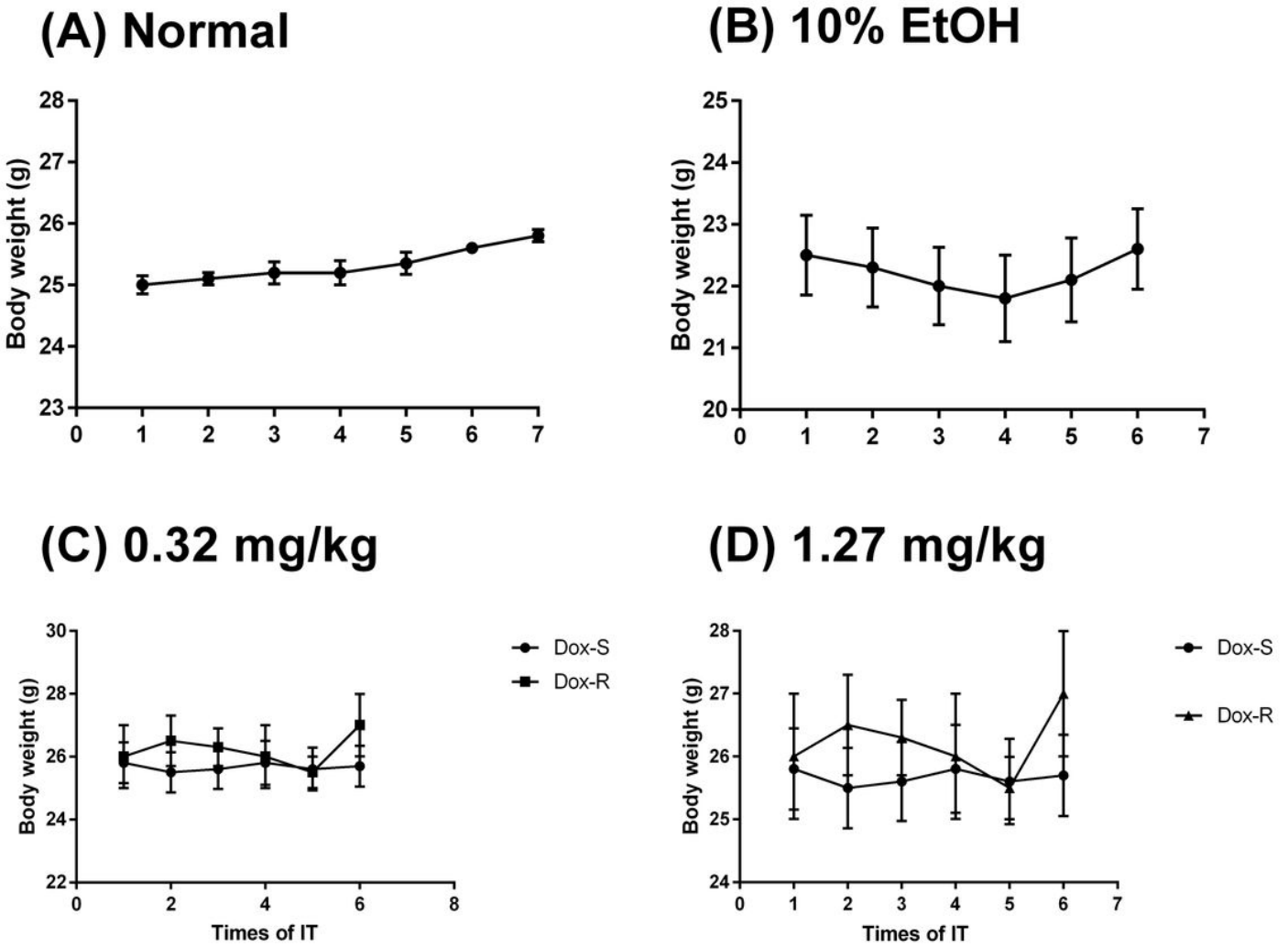


**Figure 5**

The altered body weight of cancer cell-inoculated mice during HCD treatment. Body weight of mice inoculated with Dox-S (A549) and Dox-R (Dox-R) followed by treating with (A) vehicle, (B) 10% EtOH, (C) 0.32 (100  $\mu$ M), and (D) 1.27 (400  $\mu$ M) mg/kg B. wt. of HCD, respectively, were measured at every 7 days. The scale of the X-axis was meant as the IT injection time of HCD.

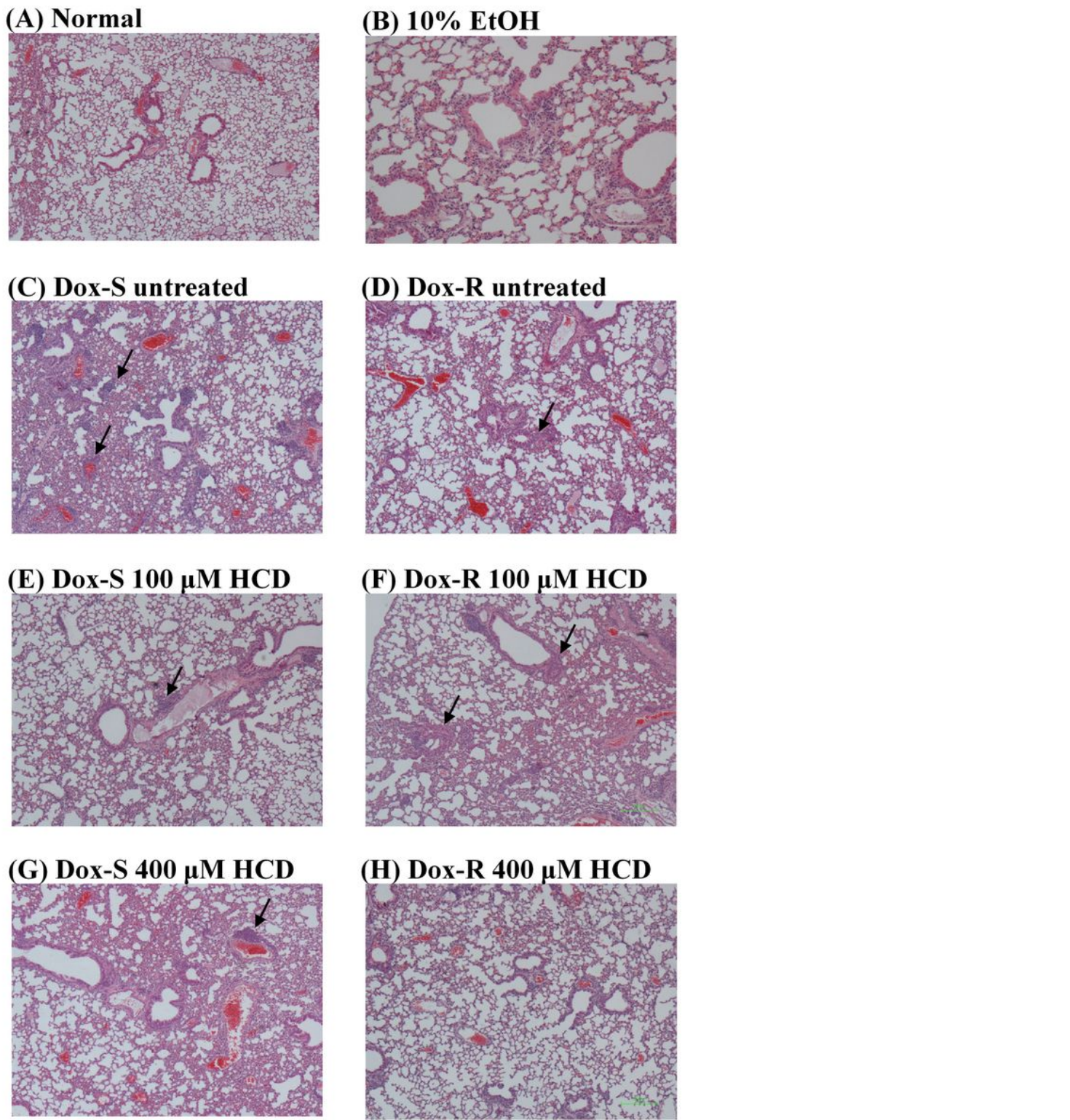


**Figure 6**

The histological changes of Dox-S and Dox-R-inoculated lung treated with HCD. Histological change of mice lung is of (A) untreated, (B) 10% EtOH, (C) Dox-S, and (D) Dox-R-inoculated before HCD treatments, and mice lung is after 0.32 mg/kg B. wt. of HCD (E, F), and 1.27 mg/kg B. wt. of HCD (G, H), respectively, were sectioned and stained with hematoxylin and eosin. (E) and (G) were section slide of Dox-S-bearing mice, and (F) and (H) were Dox-R-bearing mice. Black arrow was the position of xenograft tumor.

# Supplementary Files

This is a list of supplementary files associated with this preprint. Click to download.

- [GEL.pdf](#)
- [NC3RsARRIVEGuidelinesChecklist2014HCDA549.docx](#)